# NOVEL PROJECTOR CALIBRATION APPROACHES OF MULTI-RESOLUTION DISPLAY

Po-Hsun Chiu, [1]Shih-Yao Lin, Li-Wei Chan, Neng-Hao Yu and [2]Yi-Ping Hung,

Graduate Institute of Networking and Multimedia, National Taiwan University
E-mail: {[1]d97944010, [2]hung} @csie.ntu.edu.tw

## ABSTRACT

This paper proposes convenient and useful approaches to automatically calibrate the projectors of a multi-resolution display. The proposed approaches estimate both the keystone effect and misalignment of the projections with an assistance of a color camera. Structured light patterns are employed to construct the geometric relationship between projectors and the projection surface, and then pre-warp the images so that they appear undistorted as a result. Experimental results demonstrate that the proposed approaches successfully reduce the human-effort and lower the calibration time of multi-resolution display calibration task.

***Index Terms—***Projector Calibration; Keystone Correction; Structured Light; Rear Projection; Multi-Projector; Multi-Resolution

## 1. INTRODUCTION

Interactive display systems have been developed to bring users with more intuitive and convenient manipulation. Many studies have already engaged in this area to develop a single large-scale and high-resolution display by utilizing arrays of tiled projectors or LCD monitors. We had developed a multi-resolution display system, which is a 56-inch interactive tabletop system based on rear-projection, featuring the multi-resolution characteristics of human vision by coupling a fovea and a peripheral projection. In human eyes, fovea centralis denotes the pit in the retina which allows for maximum acuity of vision, is made use of perceiving objects at high resolution. Our system stands for the displaying area, is entirely covered by the peripheral projection of the fixed wide-angle projector.

However, the manual calibration process is usually a tedious task because it is impractical to perform fovea projector calibration for each pose manually, pose sampling is considered as an acceptable alternative. Suffering from the fact that the system performance is proportional to the number of sampled poses in calibrating the steerable fovea projector, very much human effort and time are consumed during this routine.

This paper presents an automatic calibration technique to efficiently calibrate this multi-touch and multi-resolution display system. Benefiting from it, once the display configuration is changed by some external factors (e.g. the movement of the projectors or the display surface), what we need is to re-run the proposed approach. Experimental results illustrate that our approach successfully reduces human-effort and lowers the calibration time.

## 2. RELATED WORKS

Multi-resolution is an intuitive and effective technique for large-scale and interactive display systems. To achieve this purpose, some studies provide a higher-resolution region in the central of the lower-resolution display. “Focus Plus Context Screens” [2] presented this approach by integrating a high-resolution LCD monitor into a larger low-resolution projected screen. Escritoire [3] is a similar setting was applied to the front projected tabletop system.

However, the fovea region was fixed, resulting in constraint on the user’s interaction and freedom of fovea vision. Approaches addressed on this problem were presented in “Fovea-Tablett” [5], slim tablets PCs with coded maker were put deliberately on top of tabletop surface. The positions of the tablets were tracked and the screen contents were displayed on them at higher resolution. To improve the convenience in manipulation, a fovea projector was assembled with a pan-tilt unit and a mirror to provide steerable projection [1, 4].

In above works, being set orthogonal to the display surface in “Focus Plus Context Screens” [2], the projector was aligned with the high-resolution LCD monitor and the display surface manually, and no projector calibration was performed beforehand. With simple calibration tool in the Escritoire [3] and the *i-m*-Top [1], the movement of corresponding points for geometric transformations was under control of both keyboard and mouse.

In order to achieve the purpose of automate projector calibration process, various methods have been proposed. Lee et al. [7] embedded optical sensors on the target surface at the interesting point, and utilized these sensors to measure the structured light patterns from the projector directly. For camera-based approach, Sukthankar et al. [6] calibrated a casually placed projector using planar homographies [11], and Chen et al. [8] extend this idea with a tree of homographies in calibration of a multi-projector display. However, such works were under the constraint that

geometry of the entire display surface must be planar uniformly. For dealing with arbitrary surfaces, corrected imagery would be displayed once the 3D configuration is estimated [9] shows that how to re-calibrate a multi-projector display system in real time.

## 3. SYSTEM OVERVIEW

Our approaches are based on a multi-resolution display system. With the proper calibration procedure, the system is configured with correct software setting. Thus, the developed applications on our system works the way which users desire. In this section, firstly we introduce our hardware configuration, followed with the system calibration algorithm.

### 3.1. System Environment

The diagram of our display system is illustrated in Fig. 1. The display surface employs a piece of diffuser, which is on the top of a glass sheet. A fovea projector with a pan-tilt unit (PTU), a peripheral projector, and two IR cameras with several IR LED lights are installed underneath.

The color camera (Fig. 1 (f)), which plays an important role in an automatic system calibration procedure, is mounted upon the display surface and its field of view includes the entire display. To correct the software setting as the system configuration changes (e.g. the movement of the projectors or surface), geometric calibration by observing projected structured light patterns with this color camera is performed as an off-line process. Once the calibration procedures are completed, the color camera will not be needed anymore and can be retired.

### 3.2. Stages of Calibration Algorithm

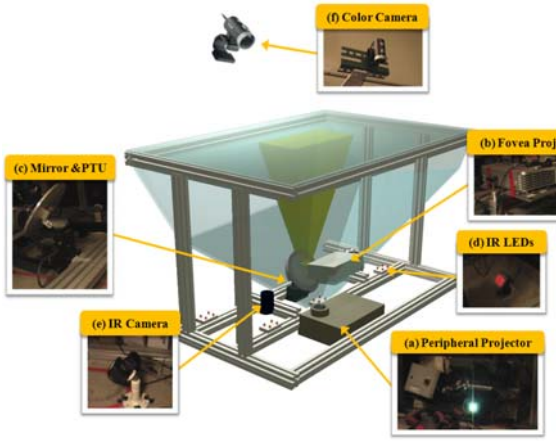


**Fig. 1.** Hardware configuration of the proposed display system (a) wide-angle peripheral projector, (b) fovea projector with (c) reflecting mirror and PTU, (d) IR LEDs, (e) two IR cameras, and (f) color camera.

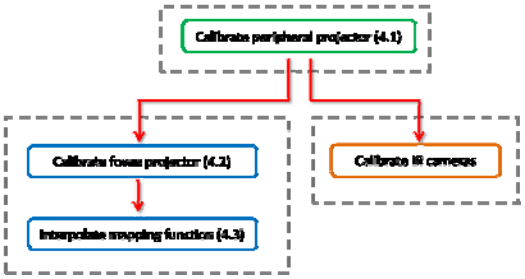


**Fig. 2.** The calibration framework of our system.

The proposed calibration algorithms calculate the transformation between the projector (peripheral projector and fovea projector) and display surface. The output of the various stages is summarized to the final result. The diagram of our calibration algorithm is shown in Fig. 2. To yield the camera image with a perfect perspective projection (pin-hole camera), the camera is pre-calibrated to deal with the radial lens distortion in advance. Camera images which capture the structured light patterns projected from peripheral projectors are then used to construct the projector-surface homography. Similar methods are adopted in calibrating the fovea projector. Now that it is impractical to do projector calibration for all valid PTU poses, we develop a calibration technique that calibrates the whole pan-tilt system by looking up the mapping table.

The proposed automatic calibration algorithms are introduced in this section. Firstly, for geometric calibration, we proposed novel projector calibration approaches, which calibrate both peripheral and fovea projector. However, the fovea projector calibration is limited to sample finite poses of PTU. By using the interpolation, we can calculate the mapping function of each non-calibrated position respectively. Then, IR camera calibration will be used to setup a correct environment for multi-touch detection as introduced below.

## 4. AUTOMATICALLY MULTI-RESOLUTION CAMERA CALIBRATION

In standard situation, it is assumed that projectors are designed to project light in a direction orthogonal to the display surface. In our system, the peripheral projector is mounted in a oblique way to supply enough space utilization. For the fovea projector, the pan-tilt mirror can reflect the projection light to anywhere over the display surface, but in most of time the display surface is oblique to the direction of projection. Due to this, the image is displayed as distorted before any pre-processing.

To integrate a high-resolution sub-region and a low-resolution display with the display surface, geometric calibration against the aforementioned distortion effect is indispensable. In order to correct the oblique projection distortion, images to be projected should undergo the pre-warping function. Our system performs a coordinate

transformation from the peripheral projector image plane (low-resolution)/fovea projector image plane (high-resolution) to the display surface plane. Mapping a 2D point in homogeneous coordinates on a plane to another plane can be achieved using a 3×3 homogeneous matrix. Unlike the peripheral projector which is fixed, the mirror which reflects the fovea projector's projection in a number of different positions as the PTU moves. It means that a different homography is required for each different PTU pose, and we will discuss how to get all homographies for all different PTU poses later. The calibration of the peripheral/fovea projector is based on the method by Sukthankar *et al.*[6]. They presented a method for calculating 2D homography matrices using a set of point correspondences in two planes.

### 4.1. Calibration of Peripheral Projector

We denote the coordinate system of color camera image plane *C*, the coordinate system of peripheral projector *PP* and the coordinate system of display surface *S*. The objective is to calculate the transformation matrix $H_{PP}^{S}$ between the peripheral projector coordinate system and the display surface coordinate system. Initially, we obtain homography $H_{C}^{S}$ and $H_{C}^{PP}$ individually, and then apply matrix multiplication to generate $H_{PP}^{S}$ . The diagram of peripheral projector calibration is illustrated in Fig. 3.

Firstly, $H_{C}^{S}$ is established using the corresponding feature points between camera image and display surface. It is claimed that the homography matrix takes at least four corresponding point pairs. Rather than placing physical markers which is inconvenient, this can be achieved by detecting the four display surface corners in camera image. Secondly, to calculate $H_{C}^{PP}$ , the homography matrix between camera and peripheral projector, some kind of feature pattern is used for associating feature point correspondences. We use a "circle pattern" (Fig. 4(a)), as the feature pattern projected by peripheral projector. The feature points can then be detected by the center of each circle. However, even though the positions of feature points are found out by using camera, we still cannot obtain the corresponding coordinate in projector space relatively. To identify each feature point, we adopt gray code patterns [12]. Fig. 4(b) shows the gray code patterns of our calibration task. By projecting these patterns, each circle in captured images can be treated as a marker with a unique address.

Due to the limitation of camera resolution, it is unable to distinguish projected imagery pixel by pixel. Discarding the pattern which has the maximum number of black/white stripes as the projector resolution, we just use enough distinguishable number of stripes to preserve time and avoid ambiguity. The pattern base is utilized as 4, indicating the number of patterns with vertical/horizontal direction. Hence there are $2^4 \times 2^4 = 256$ regions divided in projector space, and pixels belonging to one such region share the unique codeword. In feature pattern design, e.g., the circle pattern, feature point is equivalent to the center of each dividing region, matching the circle center exactly. After obtaining two homography matrices $H_{C}^{S}$ and $H_{C}^{PP}$ , these two matrices are used for calculating the homography matrix $H_{PP}^{S} = H_{C}^{S}(H_{C}^{PP})^{-1}$ . Besides the circle pattern, we employ other two categories of feature pattern. One is "concentric circle pattern", which consists of two or more circle patterns,

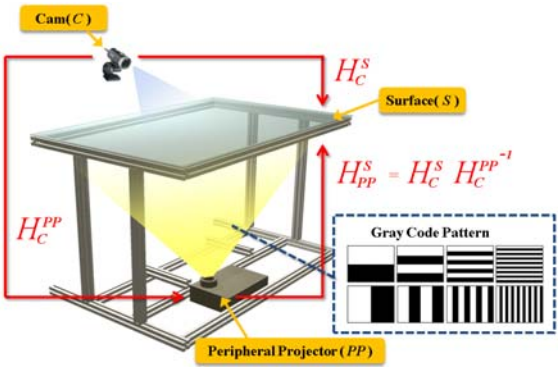


**Fig. 3.** Peripheral projector calibration.

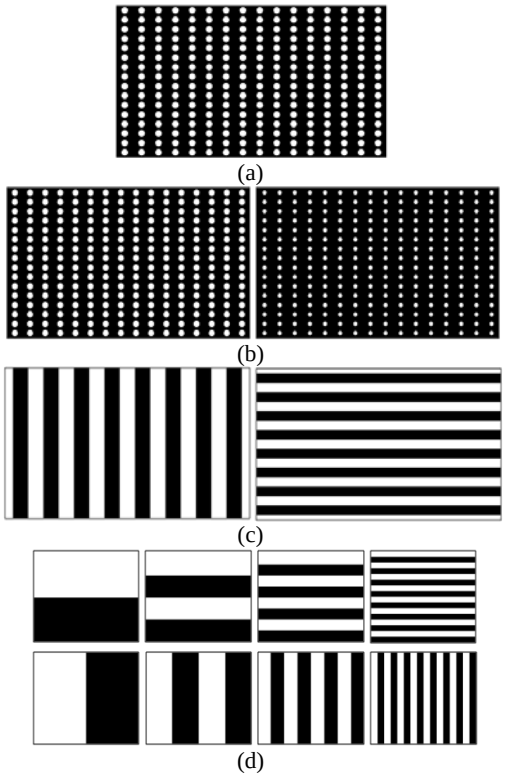


**Fig. 4.** Feature and gray code patterns. (a) Circle pattern (b) concentric circle pattern (c) middle line pattern (d) Gray code patterns.

can lead to better accuracy than merely single circle pattern. The other is “middle line pattern”. Unlike the circle or concentric circle pattern whose accuracy would drop while the circle size is reduced due to more feature points, middle line pattern overcomes this issue since its feature points are located in the intersection of pattern stripe boundaries.

### 4.2. Calibration of Fovea Projector

To calculate the transformation matrix $H_{FP}^{S}$ between the fovea projector *FP* and the display surface *S*, we follow the previous strategy in calibrating peripheral projector. Similar to peripheral projector calibration, we generate $H_{FP}^{S}$ by merging $H_{C}^{FP}$ and $H_{C}^{S}$. Given that $H_{C}^{S}$ has been estimated in previous section, thus, we only need to estimate $H_{C}^{FP}$, which is calculated in the similar way used in $H_{C}^{PP}$. The above process is applied for some desired PTU poses (pan, tilt), each corresponds to a different homography $H_{FP}^{S}$. Due to the resolution of the display surface is too high to calculate all possible homographies, which leads to a high computational cost. It is impractical to calculate the homography corresponding to each possible position of display surface. Instead we develop a calibration technique that calibrates the whole pan-tilt system which allows the fovea projector to project on any desired positions without estimating homographies sequentially for all (pan, tilt). The method is described in the next section.

### 4.3. Mapping Function Interpolation

We sampled some PTU angles with fixed interval. The movement of projection trajectories is a smooth curve, as shown in Fig. 6(a), the yellow points depict the projected position according to sampled pan-tilt poses, and the boundary of the display surface is represented by the white quadrilateral. As focusing on the movements with fixed pan (tilt) and varied tilt (pan), they can be approximated by the quadratic curves. We built a lookup table according to the calibrated PTU poses and interpolate the corresponding points for homography estimation and PTU poses for any desired display surface positions.

If we want to obtain the PTU poses of one non-calibrated position, as the red point $N_c$ shown in Fig. 6(b), first we define four quadratic lines $\{L_c^{p_1}, L_c^{p_2}, L_c^{t_1}, L_c^{t_2}\}$ surrounding it. $L_c^{p_1}$ and $L_c^{p_2}$ are fitted with four points separately, and the PTU angles correspond to each four points are fixed pan $p_1 / p_2$ and varied tilt $\{t_0, t_1, t_2, t_3\}$. Likewise, $L_c^{t_1} / L_c^{t_2}$ are defined by points with fixed tilt $t_1 / t_2$ and varied pan $\{p_0, p_1, p_2, p_3\}$ individually. After calculating the distance $\{d_0, d_1, d_2, d_3\}$ between $N_c$ and

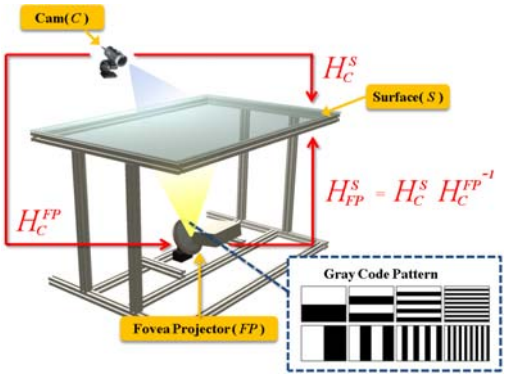


**Fig. 5.** Fovea projector calibration.

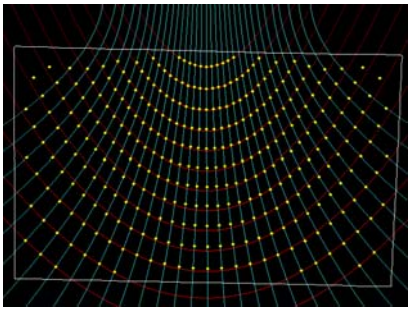

(a)

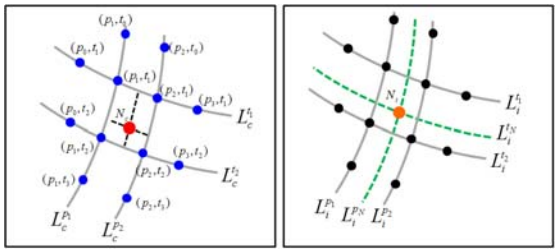

(b)

(c)

**Fig. 6.** Mapping function interpolation using lookup table: (a) quadratic curves description of moving trajectories (a) The (pan, tilt) of non-calibrated position $N_c$ is interpolated using lookup table. (b) For non-calibrated position $N_c$, the surface coordinate $N_i$ of $\{L_c^{p_1}, L_c^{p_2}, L_c^{t_1}, L_c^{t_2}\}$, the pan and tilt of $N_c$ can be calculated as follows:

$$p_N = \frac{(p_2 - p_1)}{(d_1 + d_0)} d_0 + p_1$$
$$t_N = \frac{(t_2 - t_1)}{(d_3 + d_2)} d_2 + t_1 \quad (4)$$

Secondly, we utilize the interpolated PTU pose $(p_N, t_N)$ to calculate the corresponding points for homography estimation at this non-calibrated position. From the lookup

table, there already exists the corresponding display surface and fovea projector coordinates for $H_S^{FP}$ in each calibrated PTU pose. In Fig. 6 (c), the black points are the *i*-th corresponding point associated with the twelve poses which interpolate the $(p_N, t_N)$ in previous paragraph. In the same way, these corresponding points generate another four quadratic lines $\{L_i^{p_1}, L_i^{p_2}, L_i^{t_1}, L_i^{t_2}\}$. Since we have known the fovea projector coordinate with regard to the *i*-th corresponding point, what to be estimated is the display surface coordinate for it. We first use $\{p_1, p_2, p_N\}/\{t_1, t_2, t_N\}$ and $\{L_i^{p_1}, L_i^{p_2}\}/\{L_i^{t_1}, L_i^{t_2}\}$ to interpolate two curves $L_i^{p_N}$ / $L_i^{t_N}$ as follows:

$$L_i^{p_N} = \frac{(p_N - p_1)}{(p_2 - p_1)} L_i^{p_2} + \frac{(p_2 - p_N)}{(p_2 - p_1)} L_i^{p_1}$$
$$L_i^{t_N} = \frac{(t_N - t_1)}{(t_2 - t_1)} L_i^{t_2} + \frac{(t_2 - t_N)}{(t_2 - t_1)} L_i^{t_1} \quad (5)$$

The intersection $N_i$ of $L_i^{p_N}$ and $L_i^{t_N}$, is the display surface coordinate for *i*-th corresponding point. After applying the above procedure to all corresponding points, we can therefore estimate the homography $H_S^{FP}$ and PTU pose for any position using the lookup table. In contrast to obtain the numerous parameters of such steerable projector system [10] which is complex and tedious, our approaches are more simple and general relatively.

## 5. EXPERIMENTAL RESULTS

Experimental results show the running time of calibration procedures in manual and auto mode respectively. Table 1 shows the comparison of calibration running time between manual and auto mode. In general, users cannot afford too many PTU poses. The automatic algorithm consumes no human effort and lowers the processing time.

We evaluate the error for peripheral/fovea projector calibration result, and the color camera is employed for this task. Assume the display surface is calibrated with the color camera correctly, the display surface coordinate can be transformed to the camera coordinate precisely. In our experiment, the color camera resolution is 640*480.

At the beginning, 100 testing points on the display surface are selected with random and are projected sequentially by peripheral/fovea projector. The displacement between the projected testing point which is detected by the color camera and the ground truth is viewed as error, and is divided into horizontal/vertical direction. For peripheral projector, the testing points are pre-warped before projection with the homography $H_{PP}^{S}$ and the statistical data is shown in Fig. 7(a) and Table 2. Suffering from the effect of diffuser on display surface and non-perfect control of camera exploration, middle line pattern performs not as good as imagined. However, such negative effect on circle pattern is slighter according to uniform diffusion on circles. The calibrated result of concentric circle pattern is more accurate than the result of circle pattern because of the error-reduce property. For fovea projector, we first show the calibration errors with respect to the calibrated PTU poses only. There are multiple calibration files with regard to different PTU poses. Each time we apply projected position from the calibration file which is the closest one with the present testing point. As illustrated in Fig. 7(b) and Table 2., circle pattern performs the best result.

**Table 1.** The running time in projector calibration with manual/auto mode.(*FP*: Fovea Projector, *PP*: Peripheral Projector)

| Mode | *PP* | *FP* (1 pose) | *FP* (36 poses) | *FP* (300 poses) |
|---|---|---|---|---|
| Manual | 1~2 | 1~2 min | 40~60 min | X |
| Auto | 6 sec | 6 sec | ~4.8 min | ~40 min |

**Table 2.** Calibration error for peripheral projector and fovea projector (Unit: pixel *FP*: Fovea Projector *PP*: Peripheral Projector)

| | Circle Pattern | | Concentric Circle Pattern | | Middle Line Pattern | |
|---|---|---|---|---|---|---|
| | *PP* | *FP* | *PP* | *FP* | *PP* | *FP* |
| Average | 0.112 | 0.875 | 0.180 | 0.555 | 0.455 | 0.722 |
| Standard Derivation | 0.073 | 0.468 | 0.093 | 0.398 | 0.095 | 0.178 |

Due to the limited camera resolution, the error-reduce function cannot work well in concentric circle pattern due to the fact that circle size is too small to be recognized exactly. Nevertheless, sub-pixel accuracy is achieved by our calibration algorithm for either peripheral projector or fovea projector, and the satisfactory result is presented under any kind of feature patterns. Using the result of the calibrated PTU poses, we show the interpolation result of mapping function on non-calibrated position.

As illustrated in Fig. 8(a), obviously, the accuracy of calibration results are successfully improved when the sampling interval of PTU pose become denser. However, with denser sampling interval, the processing time of entire calibration procedure increases rapidly (Fig. 8 (b) (c)). To get a balance between calibration quality and processing time, we select 64 PTU angles as the sampling interval.

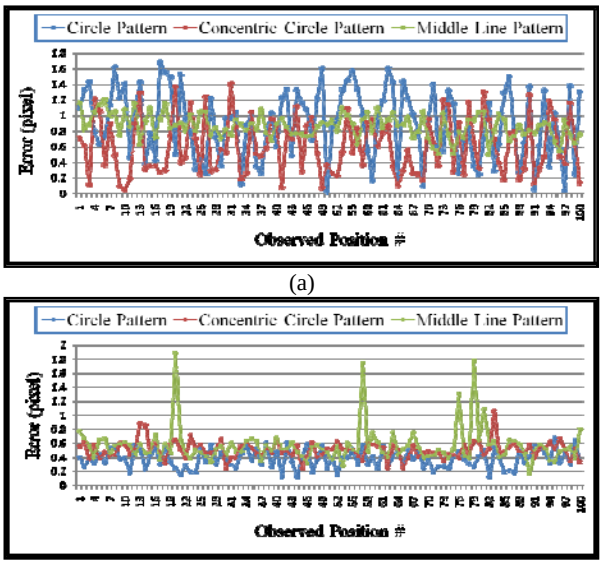


(a)




(b)

**Fig. 7.** Calibration error: (a) peripheral projector (b) fovea projector.

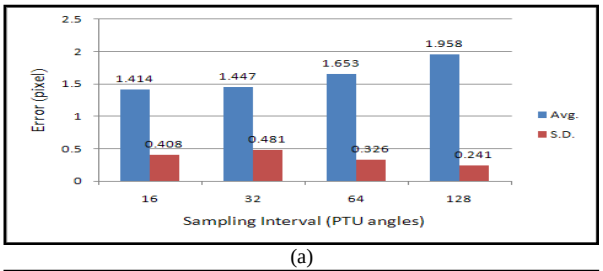


(a)

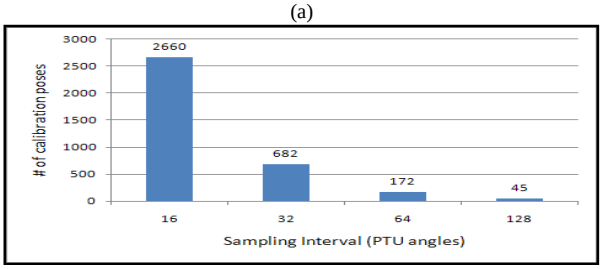


(b)

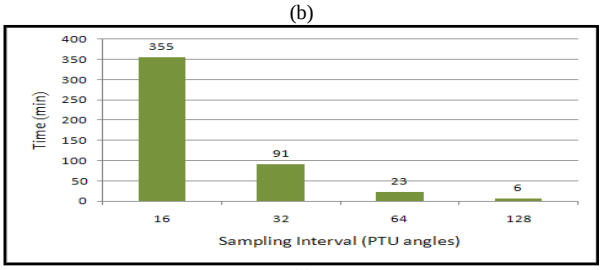


(c)

**Fig. 8.** Calibration result of fovea projector: (a) Calibration error for fovea projector (with mapping function interpolation). (b) Calibrated poses of PTU according to different sampling intervals. (c) Calibration time according to different sampling intervals of PTU.

## 6. CONCLUSIONS

We present a novel automatic calibration algorithm of multi-resolution tabletop display system for improving the performance and accuracy. Geometric transformation between projectors and the display surface is obtained by the assistance of one color camera and structured light patterns. The proposed algorithms can achieve the two objectives: (1) the keystone correction and the misalignment elimination (between the peripheral projector and fovea projector) and (2) the fovea projector is capable of projecting to the desired position on surface. The experimental results demonstrate that the proposed algorithms successfully lower the calibration error and computational cost.

## 6. ACKNOWLEDGE

This work was supported in part by the Ministry of Economic Affairs, Taiwan, under Grant 99-EC-17-A-02-S1-032, and by the National Science Council, Taiwan, under grant NSC 98-2221-E-002-128-MY3

## 7. REFERENCE

[1] T. T. Hu, Y. W. Chia, L. W. Chan, Y. P. Hung, and J. Hsu, (2008), "*i-m*-Top: An Interactive Multi-Resolution Tabletop System Accommodating to Multi-Resolution Human Vision," In 3rd IEEE TABLETOP 2008,177-180.

[2] P. Baudisch and N. Good, "Focus Plus Context Screens: Visual Context and Immersion on the Desktop," ACM SIGGRAPH 2002.

[3] M. Ashdown and P. Robinson, "Escritoire: A Personal Projected Display," In IEEE Multi-Media 2005.

[4] L.-W. Chan, W.-S. Ye, S.-C. Liao, Y.-P. Tsai, J. Hsu, and Y.-P. Hung, "A Flexible Display by Integrating a Wall-Size Display and Steerable Projectors," In Ubiquitous Intelligence and Computin 2006.

[5] J. Geisler, R. Eck, N. Rehfeld, E. Peinsipp-Byma, C. Sch¨utz, and S. Geggus, "Fovea-Tablett: A New Paradigm for the Interaction with Large Screens," In HCI (8), 2007.

[6] R. Sukthankar, R. Stockton, and M. Mullin, "Smarter Presentations: Exploiting Homography in Camera-Projector Systems," ICCV 2001.

[7] Lee, J., Dietz, P., Aminzade, D., Raskar, R., and Huedson, S, "Automatic Projector Calibration with Embedded Light Sensors," UIST 2004.

[8] H. Chen, R. Sukthankar, G. Wallace, T.-J. Cham, "Calibrating Scalable Multi-Projector Displays Using Camera Homography Trees," In CVPR Technical Sketch, 2001.

[9] R. Raskar, M. Brown, R. Yang, W. Chen, G. Welch, H. Towles, B. Seales, and H. Fuchs, "Multi-Projector Displays using Camera-Based Registration," IEEE Visualization, 1999.

[10] Mark Ashdown and Yoichi Sato, "Steerable Projector Calibration," PROCAMS 2005.

[11] R. Hartley and A. Zisserman, "Multiple View Geometry in Computer Vision 2nd edition," Cambridge University Press, 2003.

[12] J. Salvi, J. Pag`es, and J. Batlle, "Pattern Codification Strategies in Structured Light Systems," In Pattern Recognition, 37(4):827–849, 2004.